

JGR Biogeosciences

RESEARCH ARTICLE

10.1029/2020JG005844

Key Points:

- Dissolved CO₂ from a high-altitude peatland was carried into the stream and evaded to the atmosphere within the first ~150 m of the channel
- Stream CO₂ evasion was controlled mainly by geomorphic and hydrologic variables
- Aquatic CO₂ fluxes were up to an order of magnitude greater than terrestrial CO₂ fluxes in adjacent landscape positions

Correspondence to:

D. A. Riveros-Iregui,
diegori@unc.edu

Citation:

Schneider, C. L., Herrera, M., Raisle, M. L., Murray, A. R., Whitmore, K. M., Encalada, A. C., et al. (2020). Carbon dioxide (CO₂) fluxes from terrestrial and aquatic environments in a high-altitude tropical catchment. *Journal of Geophysical Research: Biogeosciences*, 125, e2020JG005844. <https://doi.org/10.1029/2020JG005844>

Received 19 MAY 2020

Accepted 7 JUL 2020

Accepted article online 27 JUL 2020

Chloe L. Schneider, Maribel Herrera, and Megan L. Raisle contributed equally to this work.

Carbon Dioxide (CO₂) Fluxes From Terrestrial and Aquatic Environments in a High-Altitude Tropical Catchment

Chloe L. Schneider¹, Maribel Herrera¹, Megan L. Raisle¹, Andrew R. Murray¹ , Keridwen M. Whitmore¹ , Andrea C. Encalada^{2,3}, Esteban Suárez³, and Diego A. Riveros-Iregui¹ 

¹Department of Geography, University of North Carolina at Chapel Hill, Chapel Hill, NC, USA, ²Laboratorio de Ecología Acuática, Universidad San Francisco de Quito, Quito, Ecuador, ³Instituto BIOSFERA and Colegio de Ciencias Ambientales, Universidad San Francisco de Quito, Quito, Ecuador

Abstract High-altitude tropical grasslands, known as “páramos,” are characterized by high solar radiation, high precipitation, and low temperature. They also exhibit some of the highest ecosystem carbon stocks per unit area on Earth. Recent observations have shown that páramos may be a net source of CO₂ to the atmosphere as a result of climate change; however, little is known about the source of this excess CO₂ in these mountainous environments or which landscape components contribute the most CO₂. We evaluated the spatial and temporal variability of surface CO₂ fluxes to the atmosphere from adjacent terrestrial and aquatic environments in a high-altitude catchment of Ecuador, based on a suite of field measurements performed during the wet season. Our findings revealed the importance of hydrologic dynamics in regulating the magnitude and likely fate of dissolved carbon in the stream. While headwater catchments are known to contribute disproportionately larger amounts of carbon to the atmosphere than their downstream counterparts, our study highlights the spatial heterogeneity of CO₂ fluxes within and between aquatic and terrestrial landscape elements in headwater catchments of complex topography. Our findings revealed that CO₂ evasion from stream surfaces was up to an order of magnitude greater than soil CO₂ efflux from the adjacent terrestrial environment. Stream carbon flux to the atmosphere appeared to be transport limited (i.e., controlled by flow characteristics, turbulent flow, and water velocity) in the upper reaches of the stream, and source limited (i.e., controlled by CO₂ and carbon availability) in the lower reaches of the stream. A 4-m waterfall along the channel accounted for up to 35% of the total evasion observed along a 250-m stream reach. These findings represent a first step in understanding ecosystem carbon cycling at the interface of terrestrial and aquatic ecosystems in high-altitude, tropical, headwater catchments.

Plain Language Summary Mountain streams are a critical part of the global carbon cycle. Multiple studies have highlighted this importance in different regions around the globe, and some have shown that mountain streams are a significant source of carbon dioxide emissions. The Tropical Andes are unique because of proximity to the equator, high elevation, and high rainfall. We studied a high-altitude, tropical grassland ecosystem known as a “páramo,” which contains some of the highest carbon stocks on Earth. Our results demonstrate that hydrologic connectivity between wetlands and streams is critical for the movement of carbon downstream and also for the emissions of carbon to the atmosphere. Our study highlights that hydrologic dynamics play an important role in determining the amount and the fate of dissolved carbon within the stream as well as the spatial differences in carbon emissions across the aquatic-terrestrial interface. These results represent a first step in understanding ecosystem-level carbon cycling between wetland and stream ecosystems in high-altitude, tropical, headwater catchments.

1. Introduction

A rapidly growing body of work recognizes inland waters as fundamental players in the carbon cycle (Bastviken et al., 2011; Butman & Raymond, 2011; Hotchkiss et al., 2015; Raymond et al., 2013). In particular, headwater streams have been the focus of recent scientific investigations because they connect terrestrial and aquatic ecosystems, having a higher proportion of stream water volume in direct contact with adjacent

soils (Argerich et al., 2016; Benstead & Leigh, 2012). Headwater streams receive and transform terrestrial carbon, emitting greenhouse gases such as CO₂ into the atmosphere, and transporting dissolved organic, inorganic, or particulate carbon downstream (Aufdenkampe et al., 2011; Battin et al., 2008). Headwater streams comprise over 80% of the total length of all perennial channels (Downing et al., 2012; Vannote et al., 1980), and recent investigations suggest that the surface area of these streams is much greater than previously thought, particularly in areas with dense stream networks such as the Andean-Amazon basin where stream surface area has been underestimated by up to 67% (Allen & Pavelsky, 2018).

While the importance of headwater streams in the global carbon cycle seems clear today, CO₂ effluxes from headwater catchments are poorly characterized. Studies that quantify CO₂ fluxes from aquatic environments traditionally focus on one type of aquatic system (i.e., wetland, stream, and lake), keeping with a long tradition of intellectual separation among lake, stream, and wetland science (Stanley & del Giorgio, 2018). The result is a disconnect in our understanding of how hydrologic processes affect whole-ecosystem C fluxes across the continuum from terrestrial to aquatic systems. Current estimates suggest that the fate of terrestrial C entering aquatic systems involves mainly two large fluxes: direct loss of aquatic C to the atmosphere and downstream export (Cole et al., 2007; Ward et al., 2017); only a small fraction of the terrestrial C input is stored in aquatic sediments. A recent cross-ecosystem review by Webb et al. (2019) integrated aquatic and terrestrial fluxes at the catchment scale on an annual basis and across a broad latitudinal gradient. Two important themes emerged after the Webb et al. (2019) study. The first is that aquatic C fluxes represent a wide range of the total net ecosystem carbon budget across different ecosystems (e.g., forests, wetlands, and agrosystems). The second theme is that the role of hydrologic processes in contributing to the variability of such aquatic C fluxes may be as wide and varied as the ecosystems themselves. For instance, at the continental scale, Hotchkiss et al. (2015) suggested that the relative role of rivers as conduits for terrestrial CO₂ efflux is a function of their size as well as their connectivity with landscapes. The same researchers suggested that for some rivers, hydrologic connectivity with floodplains might be more important than discharge, stream order, or other size-based attributes. At the scale of single catchments, connectivity between streams and nearby soils is known to facilitate the delivery of dissolved carbon to the stream (Pacific et al., 2010). However, factors such as topography and hydrologic dynamics are known to mediate the spatial patterns of greenhouse gas fluxes from terrestrial environments to the atmosphere (Riveros-Iregui & McGlynn, 2009; Riveros-Iregui, McGlynn, et al., 2011). To the best of our knowledge, a comparison of CO₂ effluxes from different landscape elements, including adjacent terrestrial and aquatic environments, and in the context of hydrologic variability is lacking.

Recent investigations have highlighted the role of mountainous environments in global carbon fluxes, as CO₂ fluxes from mountain streams can equal or exceed those from lowland tropical environments or boreal streams (Horgby, Segatto, et al., 2019). One region that has remained absent from direct observations in mountain environments are the Tropical Andes, particularly at the highest elevations (Riveros-Iregui et al., 2018). These are regions known to be important carbon stores due to unique combinations of environmental variables, including high solar radiation, high precipitation, and low temperature. In fact, high-altitude tropical grasslands known as “páramos” exhibit some of the highest rates of ecosystem carbon storage per unit area on Earth (30% by volume; Hribljan et al., 2017), notwithstanding that their geographic extent along the Andes is small (from 35,000 to 77,000 km²; Buytaert et al., 2006; Luteyn, 1999). Field observations from páramos have shown that, at the ecosystem level, these high-altitude grasslands may act as a net source of CO₂ to the atmosphere, likely as a result of ongoing climate change (Carrillo-Rojas et al., 2019). However, little is known about the source of this excess CO₂ in these mountainous environments or whether specific landscape positions may be disproportionately contributing more CO₂ to the atmosphere than others.

In this paper, we evaluated the spatial and temporal variability of surface CO₂ fluxes from adjacent terrestrial and aquatic environments in high-altitude, tropical environments. We report on direct observations conducted over 7 weeks of the wet season in a small páramo catchment in northern Ecuador with strong geomorphic gradients. We provide a comparison of terrestrial and aquatic CO₂ fluxes from diel to seasonal time scales with a threefold goal: (1) to quantify CO₂ fluxes to the atmosphere from adjacent aquatic-terrestrial ecosystems, (2) to evaluate the longitudinal change of aquatic CO₂ fluxes to the atmosphere, and (3) to provide a field evaluation of CO₂ fluxes to the atmosphere across wetland-stream transitions. This new

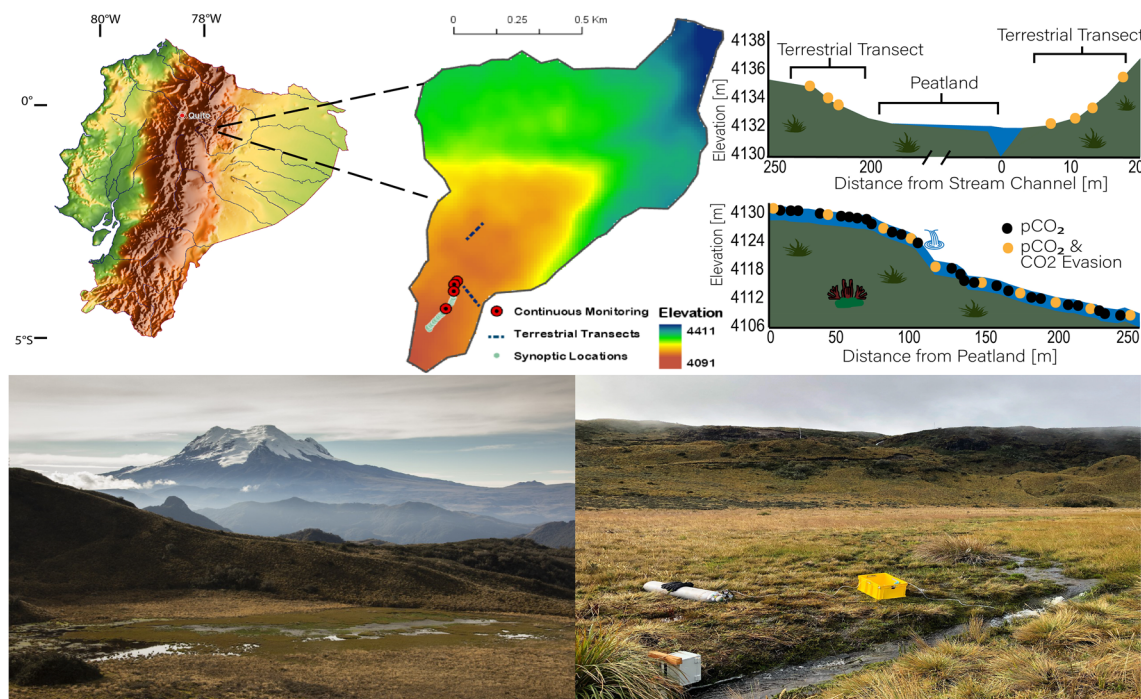


Figure 1. (top left) The map of Ecuador was produced by the GinkoMaps project (<https://www.ginkomaps.com>). (top center) Digital elevation model of the study catchment, located in the Cayambe-Coca Ecological Reserve. (top right) Sampling locations across the terrestrial and aquatic environments, which included soil CO₂ efflux (terrestrial) and $p\text{CO}_2$ and CO₂ observations (aquatic). Bottom panels depict photographs of the study site, including peatland with Antisana Volcano in the background (bottom left) and peatland outlet (bottom right).

understanding is needed to better constrain estimates of CO₂ effluxes from heterogeneous, headwater catchments in high-altitude tropical regions.

2. Methods

2.1. Study Site

Our research site was located in the Cayambe-Coca National Park, a páramo ecoregion in the northern Ecuadorian Andes (elevation 4,130 m). This páramo ecosystem exhibits a mean daily temperature of 5°C and a mean annual precipitation of 1,375 mm (Sánchez et al., 2017). The study watershed was a headwater catchment delimited to the west by the continental divide of the Andes Mountains, and draining to the east toward the Napo and Amazon Rivers. The site is characterized by high-altitude wetland and peatland complexes that are connected by well-defined, incised stream channels. Land cover at this site consists of páramo vegetation communities, including grassland, scrublands, and small pockets of high Andean forests and dense shrubs. Vegetation in the hillslopes includes *Calamagrostis intermedia*, *Diplostephium* spp., *Loricaria* spp., and *Hypericum laricifolium*. We focused on a 2.3-ha peatland (hereafter peatland) drained by a single outlet on the south end and into a stream channel cutting through complex topography (Figure 1). Vegetation in this peatland is dominated by *Carex lemanniana*, *Calamagrostis ligulata*, and *Eleocharis* sp. The outlet stream flowed NNE-SSW, of which the first 250 m was selected as the stream reach for this study (hereafter stream reach). This stream reach was divided into upper and lower portions by a 4-m waterfall located 107 m downstream from the peatland outlet (Figure 1). Mean peatland soil depth for the region is 4.6 m, with a mean estimated storage of 2,100 Mg C ha⁻¹, believed to be at least 3,000 years old (Hribljan et al., 2016, 2017).

2.2. Environmental Variables

We evaluated the spatial and temporal variability of CO₂ effluxes to the atmosphere from this headwater catchment, based on a suite of field measurements performed from 1 July to 16 August 2019; this period is typically the beginning of the wet season for the region (Sklenář & Lægaard, 2003). Precipitation was

recorded every 5 min at a weather station located ~1 km to the south (Station No. M5025, Lat: -0.33° , Long: -78.19°), which is part of the Hydroclimatic Stations Network of the Fund for the Protection of Water (FONAG), a member of the Latin American Water Funds Partnership.

Water level was collected from two permanently deployed in-stream water level loggers along the channel (Model 3001, Solinst Canada Ltd., Georgetown, Ontario), collecting observations every 15 min. Dissolved oxygen (DO) was collected using DO sensors (HOBO Dissolved Oxygen Level Logger, Onset Computer Corporation, Bourne, Massachusetts) every 15 min. Level-discharge rating curves were developed by collecting velocity, depth, and width measurements of vertical segments across the stream cross section and adding discharges for all segments. Velocity measurements were collected using a current meter (Model FP101, Global Flow Probe, Global Water, Gold River, California). Rating curves were based on 40 discharge measurements collected over the course of the study period. Discharge is reported in ($\text{m}^3 \text{ s}^{-1}$).

2.3. Aquatic Fluxes: $p\text{CO}_2$, CO_2 Evasion, and Other Aquatic Variables

We report on continuous and discrete observations of several variables collected throughout our site. Four stations were established in the stream reach at 6.2 m (Station 1), 26 m (Station 2), 56 m (Station 3), and 140 m (Station 4) downstream from the peatland outlet. Each station was equipped with a solid-state CO_2 sensor (GMP222 with transmitter, Vaisala, Helsinki, Finland) installed at the bottom of the stream measuring dissolved CO_2 ($p\text{CO}_2$) at 15-min intervals and logging to a datalogger (OM-CP-VOLT101A-2.5 V, Omega Engineering Inc., Norwalk, Connecticut). The solid-state sensors were adapted for wet environments as in Johnson et al. (2010), and all measurements were corrected following pressure and temperature compensatory procedures described by the manufacturer in the manual. Along with the CO_2 probes, two water-level loggers were placed at Stations 1 and 3, and three DO sensors were placed at Stations 1, 2, and 4.

We deployed two EosFD flux chambers (EosFD, Eosense Inc., Dartmouth, Nova Scotia Canada) to estimate soil CO_2 efflux and CO_2 evasion. Because the EosFD was developed for measurements over the soil (Risk et al., 2011), we adapted one unit for continuous measurements of CO_2 evasion from the water surface using a floating platform collar open at the bottom that allowed for minimum disruption of streamflow while trapping CO_2 evaded from the water surface under most levels of streamflow. The floating platform was constructed from a semirigid plastic disk with a 61-cm diameter fastened to two “pontoons” made of 6.35-cm diameter PVC pipe. The pontoons were cut to ~61-cm lengths and capped to provide flotation and angled in a “V” configuration so that they would not create turbulent conditions of water flowing under the disk and eosFD. In addition, the disk was fitted with a PVC collar in the center, allowing the eosFD to fit snuggly onto one end while the other end dipped approximately 3 cm below the water surface when floating in the stream. A C6 Multi-Sensor (C6 Multi-Sensor Platform, Turner Designs Inc., San Jose, California) was deployed between Stations 1 and 2, 10 m downstream from the peatland outlet, to collect measurements of turbidity, chlorophyll A, and colored dissolved organic matter (CDOM). This C6 sensor was calibrated in the lab according to the manufacturer’s instructions prior to deployment, with one final calibration in situ to adjust for local elevation and atmospheric pressure. The C6 was initially deployed at a depth of 20 cm below the water surface, but this depth ranged between 5 and 45 cm with changing water stage.

In addition to the continuous $p\text{CO}_2$ observations at the four stations, we collected synoptic observations at 35 locations along the 250-m reach on six different days throughout the study period. These sampling campaigns included manual measurements of $p\text{CO}_2$ using a handheld probe (GM70 Hand-held, Vaisala, Helsinki, Finland) at spatial intervals ranging from 2 to 10 m ($n = 35$), and measurements of CO_2 evasion at spatial intervals ranging from 10 to 35 m ($n = 10$). The $p\text{CO}_2$ observations measured by the GM70 probe were corrected for temperature and pressure following compensatory procedures described by the manufacturer in the manual. To measure CO_2 evasion, the EosFD chamber was secured to a rebar post, which was inserted into the bottom of the streambed so that the bottom of the EosFD chamber was flush with the surface of the water. This design was intended to minimally disrupt flow while creating a seal preventing atmospheric air from entering the chamber while measurements were being conducted. Three CO_2 evasion measurements were collected at each site at 5-min intervals for a total of 15 min per site. Synoptic observations were conducted on 18, 25, 29, and 31 July and 6 and 12 August with the goal of capturing the dynamics of $p\text{CO}_2$ and CO_2 evasion under different hydrologic conditions.

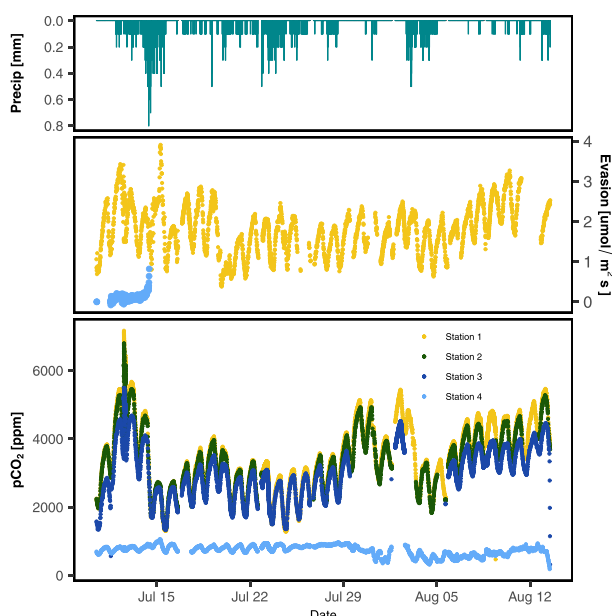


Figure 2. Continuous observations of rainfall (5 min), CO_2 evasion (15 min), and dissolved CO_2 ($p\text{CO}_2$; 15 min) collected at monitoring four stations along the stream channel.

2.4. Terrestrial Fluxes: Soil CO_2 Efflux

Two transects were established on hillslopes adjacent to the peatland, along a soil moisture gradient imposed by topography that exhibited various degrees of saturation. The first transect was established north of the peatland (i.e., opposite end from the peatland outlet), with three permanent plots starting at the edge of the peatland and extending into the adjacent hillslope. The second transect was established to the southeast of the peatland, with four permanent plots starting at the edge of the peatland and extending into the adjacent hillslope. In each transect plot, a PVC collar was inserted approximately 1 cm into the soil and the vegetation was carefully removed from the enclosed area as in Riveros-Iregui and McGlynn (2009). Due to the known challenges of overestimation of soil moisture in organic soils using traditional field soil moisture sensors (Pacific et al., 2008), soil moisture was not volumetrically measured and instead it was only characterized by the level of saturation of the soil, divided into either “saturated” or “unsaturated” based on whether standing water was present. Flux was measured by placing the EosFD flux chamber over each collar and allowing for sampling for 15 min at 5-min intervals, for a total of three soil CO_2 efflux measurements per plot. Results are reported as the mean and one standard deviation of the three measurements.

2.5. Isotopic Analysis of Soil CO_2 Efflux and CO_2 Evasion

Air samples for isotopic analysis were collected during four synoptic campaign days along the stream reach, and during four additional days from the two hillslope transects. The aforementioned PVC collars were adapted for manual sampling of their headspace with Nalgene tubing installed through the side, sealed, and fitted with a stopcock valve. On sampling days, 120 ml of headspace air were extracted from each PVC collar with a syringe over a period of 2 min, following Liang et al. (2016). Gas extraction was conducted while the EosFD chamber was deployed and circulating air, and once all EosFD measurements had been completed. The samples were immediately transferred into 1-L Tedlar bags (Standard FlexFoil Air Sample Bags, SKC Inc., Eighty Four, Pennsylvania) and taken to the lab for analysis.

Within 24 hr of collection, Tedlar bags were connected to a Cavity Ring-Down Spectroscopy (CRDS) analyzer (Model 2101-i Picarro Inc., Santa Clara, California) to measure the $\delta^{13}\text{C}$ composition of CO_2 in soil efflux and evasion. The CRDS analyzer was routinely calibrated following manufacturer's recommendations in a lab at the Universidad de San Francisco de Quito and according to protocols described in Liang et al. (2016). Working standards were created in-lab using a purchased NOAA Global Monitoring Division certified CO_2 standard. The measured precision of the standard gas was better than 0.2‰ from 20 repeated measurements.

3. Results

3.1. Environmental Variables

Variability of precipitation is summarized in Figure 2 (top panel). During the seven-week study period, the site received 340 mm of rainfall with a maximum daily value of 38.2 mm on 14 July 2019. This maximum value was also the largest daily rainfall amount recorded at this site since 2012. During the study period, over half of the days (60%) received less than 6 mm of rainfall, while the historic record shows that, since 2010, 88% of days have received at least 0.2 mm of rainfall. Average daily temperature was 2.9°C, with a daily maximum of 5.5°C and a daily minimum of 1.4°C. The highest temperature recorded during the study period was 12°C on 3 July, whereas the lowest temperature was -2.2°C recorded on 14 August. Discharge in the stream reach ranged by over an order of magnitude, from 0.0025 m^3/s on 12 August to 0.06 m^3/s on 14 July 2019.

3.2. Aquatic Fluxes: $p\text{CO}_2$, CO_2 Evasion, and Other Aquatic Variables

Continuous measurements collected at Stations 1, 2, and 3 showed an increase in $p\text{CO}_2$ over periods of low precipitation and a decrease in $p\text{CO}_2$ following precipitation events (Figure 2, bottom panel). In general,

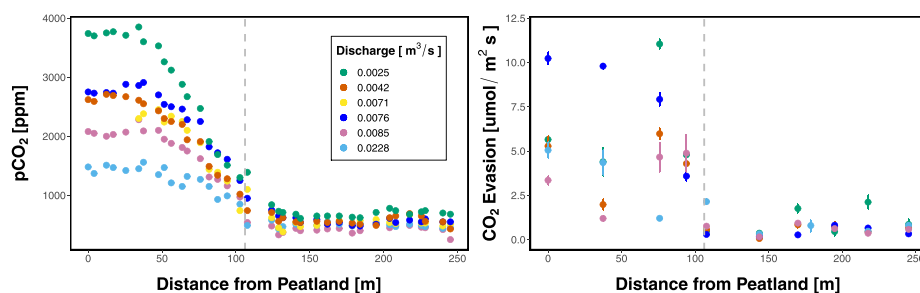


Figure 3. Dissolved CO_2 ($p\text{CO}_2$; left) and CO_2 evasion (right) measured over six different days in relation to the outlet of the 2.3-ha peatland. Different colors represent the different days in which these synoptic observations were conducted and the measured discharge on each day. The dashed lines denote the location a 4-m waterfall along the stream channel.

$p\text{CO}_2$ across Stations 1, 2, and 3 was similar in magnitude and temporal behavior, varying by at least 1,000 ppm over the course of a day and ranging from 1,000 to over 4,000 ppm over the study period. In contrast, $p\text{CO}_2$ measured below the waterfall at Station 4 was much lower in magnitude, varying by less than 100 ppm over the course of a day and ranging from 250 to 750 ppm over the study period. CO_2 evasion measured continuously at Station 1 varied by approximately $1.5 \mu\text{mol m}^{-2} \text{ s}^{-1}$ on a diel basis, ranging from 0.5 to $3.5 \mu\text{mol m}^{-2} \text{ s}^{-1}$ over the study period (Figure 2, middle panel). Measurements of CO_2 evasion at Station 4 were conducted for only a few days before a large storm event permanently damaged our sampling setup. During these few days, CO_2 evasion at Station 4 ranged from close to 0 to $0.8 \mu\text{mol m}^{-2} \text{ s}^{-1}$, and it appears that CO_2 evasion was increasing rapidly as discharge increased during the storm.

Discrete observations along the stream reach revealed that $p\text{CO}_2$ and CO_2 evasion were higher near the outlet of the peatland and progressively decreased downstream (Figure 3). This pattern was consistent over all six synoptic campaigns, with $p\text{CO}_2$ decreasing from 3,850 ppm near the outlet of the peatland to ~ 400 ppm at the most downstream portion of the stream reach (250 m downstream). After the rapid decrease of $p\text{CO}_2$ in the upper 125 m of the stream, $p\text{CO}_2$ remained relatively constant for the remaining 125 m of the stream reach. CO_2 evasion followed a similar decreasing trend in the downstream direction although not as well defined as $p\text{CO}_2$, particularly within the upper portion of the stream. For the upper 125 m of the stream

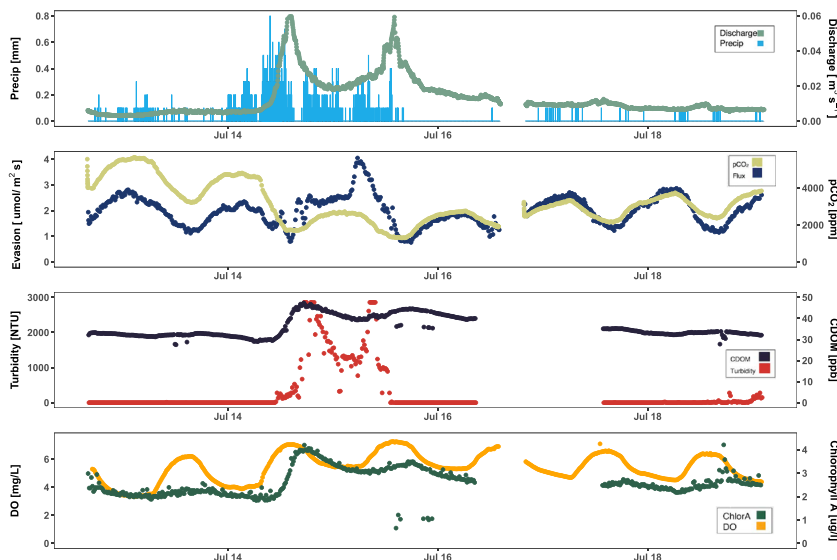


Figure 4. Continuous observations (15-min) of discharge, $p\text{CO}_2$, CO_2 evasion, turbidity, colored dissolved organic matter (CDOM), chlorophyll A, and dissolved oxygen (DO) collected 18 m downstream from outlet over a 6-day period that included a record-setting rainfall event (14 July).

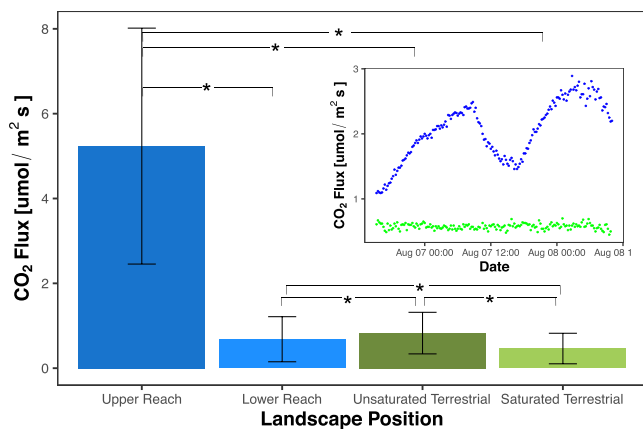


Figure 5. Variability of CO₂ fluxes according to landscape position, including upper stream reach ($n = 75$), lower stream reach ($n = 114$), unsaturated terrestrial locations ($n = 108$), and saturated terrestrial environment ($n = 83$). Bars denote the mean and standard deviation of all measurements collected in both the terrestrial and aquatic environments. Asterisks denote statistically significant differences ($p < 0.01$). Inset represents a 40-hr period during which CO₂ flux was concurrently measured in the upper reach of the stream (blue; ~18 m from the outlet of the peatland) and in the adjacent stream bank characterized with saturated soil (green).

reach, CO₂ evasion ranged from 1.2 to 10.6 $\mu\text{mol m}^{-2} \text{s}^{-1}$, whereas for the lower 125 m of the reach CO₂ evasion ranged from 0.06 to 2.1 $\mu\text{mol m}^{-2} \text{s}^{-1}$. Discharge was inversely proportional to the magnitude of $p\text{CO}_2$ leaving the peatland (i.e., greater $p\text{CO}_2$ at low discharge and lower $p\text{CO}_2$ at high discharge). The $p\text{CO}_2$ values recorded on the day of highest discharge (0.0228 $\text{m}^3 \text{s}^{-1}$) decreased from 1,560 to 430 ppm along the stream reach. In contrast, $p\text{CO}_2$ values recorded on the day of the lowest discharge (0.0025 $\text{m}^3 \text{s}^{-1}$) decreased from 3,850 to 610 ppm along the same distance (Figure 3).

Continuous observations collected near the outlet of the peatland before and after the storm on 14 July showed that the increase in discharge was accompanied by a synchronous decrease of $p\text{CO}_2$ in the stream, and by a lagged, short-lived increase in CO₂ evasion (Figure 4). Prior to the storm, turbidity was near 0 NTU but increased rapidly with discharge, whereas CDOM, DO, and chlorophyll A also responded to increases in discharge but maintained their diel dynamics. Both $p\text{CO}_2$ and CO₂ evasion reached a daily maximum between 0300 and 0500 local time (LT) and a daily minimum between 1400 and 1600 LT consistently throughout the study period. In contrast, CDOM, DO, and chlorophyll A all reached a daily maximum between 1500 and 1700 LT, and a daily minimum did not occur during a consistent time period.

3.3. Terrestrial Fluxes: Soil CO₂ Efflux

The average CO₂ efflux from unsaturated soil was 0.83 $\mu\text{mol m}^{-2} \text{s}^{-1}$, whereas CO₂ efflux from saturated soil was 0.46 $\mu\text{mol m}^{-2} \text{s}^{-1}$ (Figure 5). For comparison, the average CO₂ evasion flux measured in the upper 100 m of the stream reach was 5.24 $\mu\text{mol m}^{-2} \text{s}^{-1}$, about 7.7 times higher than that of the lower portion of the stream reach (0.68 $\mu\text{mol m}^{-2} \text{s}^{-1}$). Overall, mean soil CO₂ efflux was greater ($p < 0.001$; Wilcoxon Rank Sum and two-sampled t test) in unsaturated soils ($n = 108$) than in saturated soils ($n = 83$). However, regardless of saturation, mean soil CO₂ efflux was lower ($p < 0.001$) than mean CO₂ evasion from the upper stream reach ($n = 75$). CO₂ evasion from the lower stream reach ($n = 114$) was lower than soil CO₂

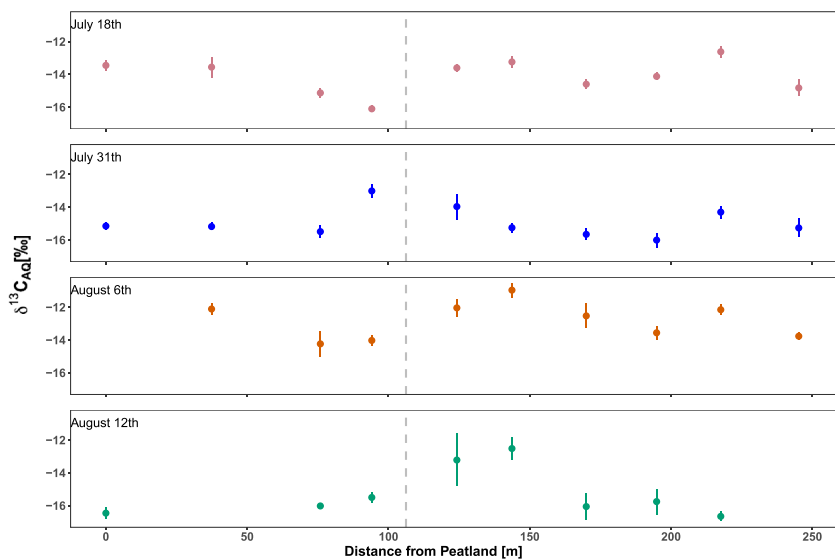


Figure 6. The $\delta^{13}\text{C}$ composition of CO₂ evasion ($\delta^{13}\text{C}_{\text{AQ}}$) collected from the surface water during four synoptic campaigns and graphed as a function of distance from the peatland outlet. Symbol colors correspond with discharge values in Figure 3. The dashed lines denote the location a 4-m waterfall along the stream channel.

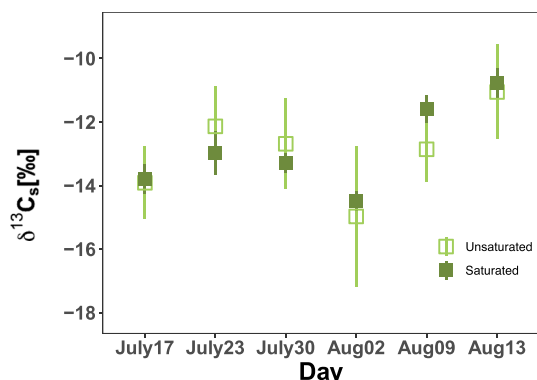


Figure 7. The $\delta^{13}\text{C}$ composition of CO_2 efflux ($\delta^{13}\text{C}_S$) collected from the soil surface, including unsaturated and saturated locations. Data points represent the mean and one standard deviation of all measurements.

efflux ($\delta^{13}\text{C}_S$) collected from soil collars is shown in Figure 7, separated into saturated and unsaturated areas. The $\delta^{13}\text{C}_S$ ranged from $-9.7\text{\textperthousand}$ to $-18.0\text{\textperthousand}$, with unsaturated collars showing more negative values ($-10.6\text{\textperthousand}$ to $-18.0\text{\textperthousand}$) than saturated collars ($-9.7\text{\textperthousand}$ to $-14.3\text{\textperthousand}$). We found significant differences between means of $\delta^{13}\text{C}_{\text{AQ}}$ and $\delta^{13}\text{C}_S$ ($p < 0.05$; Wilcoxon Rank Sum and two-sampled t test), but no significant differences were found between $\delta^{13}\text{C}_S$ of saturated and unsaturated locations.

Finally, an interesting finding emerged when evaluating the relationship between $p\text{CO}_2$ and $\delta^{13}\text{C}_{\text{AQ}}$ in the context of position within the stream reach. Stream reach locations closer to the peatland outlet had higher $p\text{CO}_2$ concentrations and more negative $\delta^{13}\text{C}_{\text{AQ}}$ values (Figure 8) than those locations farther from the peatland outlet. As distance from the outlet increased, $p\text{CO}_2$ decreased and $\delta^{13}\text{C}_{\text{AQ}}$ became more variable, exhibiting some highly enriched values.

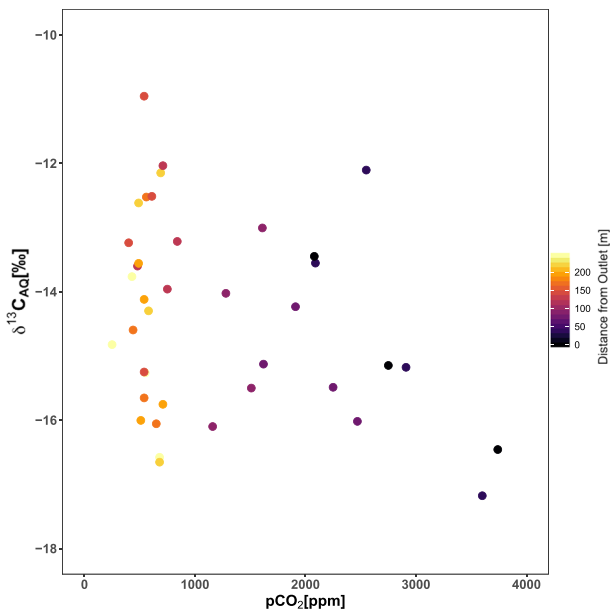


Figure 8. Variability in the $\delta^{13}\text{C}$ composition of CO_2 evasion ($\delta^{13}\text{C}_{\text{AQ}}$) in relation to that of dissolved CO_2 ($p\text{CO}_2$). Symbol color denotes distance from the peatland outlet.

efflux from unsaturated soils ($p < 0.01$) but greater than soil CO_2 efflux from saturated soils ($p < 0.001$). Finally, we observed differences in the diel dynamics of soil CO_2 efflux compared to CO_2 evasion from the stream (Figure 5, inset). CO_2 evasion ranged from ~ 1 to $2.9 \mu\text{mol m}^{-2} \text{ s}^{-1}$ with well-defined diel patterns, whereas soil CO_2 efflux from saturated soils ranged from 0.2 to $0.4 \mu\text{mol m}^{-2} \text{ s}^{-1}$ with no sign of diel variability.

3.4. Isotopic Analysis of Soil CO_2 Efflux and CO_2 Evasion

The $\delta^{13}\text{C}$ composition of CO_2 evasion from the stream ($\delta^{13}\text{C}_{\text{AQ}}$) was measured over four synoptic campaigns ($n = 37$). The $\delta^{13}\text{C}_{\text{AQ}}$ across all samples ranged from $-10.9\text{\textperthousand}$ to $-17.2\text{\textperthousand}$ (Figure 6). In general, the highest observed $\delta^{13}\text{C}_{\text{AQ}}$ along the stream reach was in the vicinity of the waterfall occurring at 107 m downstream of the outlet. However, no other apparent spatial pattern was observed along the stream reach. On the other hand, the variability in $\delta^{13}\text{C}$ of soil CO_2

efflux ($\delta^{13}\text{C}_S$) collected from soil collars is shown in Figure 7, separated into saturated and unsaturated areas. The $\delta^{13}\text{C}_S$ ranged from $-9.7\text{\textperthousand}$ to $-18.0\text{\textperthousand}$, with unsaturated collars showing more negative values ($-10.6\text{\textperthousand}$ to $-18.0\text{\textperthousand}$) than saturated collars ($-9.7\text{\textperthousand}$ to $-14.3\text{\textperthousand}$). We found significant differences between means of $\delta^{13}\text{C}_{\text{AQ}}$ and $\delta^{13}\text{C}_S$ ($p < 0.05$; Wilcoxon Rank Sum and two-sampled t test), but no significant differences were found between $\delta^{13}\text{C}_S$ of saturated and unsaturated locations.

Finally, an interesting finding emerged when evaluating the relationship between $p\text{CO}_2$ and $\delta^{13}\text{C}_{\text{AQ}}$ in the context of position within the stream reach. Stream reach locations closer to the peatland outlet had higher $p\text{CO}_2$ concentrations and more negative $\delta^{13}\text{C}_{\text{AQ}}$ values (Figure 8) than those locations farther from the peatland outlet. As distance from the outlet increased, $p\text{CO}_2$ decreased and $\delta^{13}\text{C}_{\text{AQ}}$ became more variable, exhibiting some highly enriched values.

4. Discussion

4.1. Are High-Altitude Tropical Peatlands Important Contributors of Greenhouse Gases to the Atmosphere?

We observed that dissolved CO_2 generated in this high-altitude, tropical peatland was carried into the stream reach where over 80% of it was evaded to the atmosphere within the first ~ 150 m of the channel (Figures 2 and 3), regardless of stream discharge. These results suggest that high-altitude tropical peatlands may act as sources of dissolved CO_2 to the stream network via lateral transport, at least while hydrologic connectivity between the peatland and the stream allows for the mobilization of dissolved carbon downstream (e.g., during the wet season). Wetlands store high amounts of organic matter and emit high fluxes of CO_2 and CH_4 to the atmosphere (Schelker et al., 2016). While freshwater wetlands are predominantly understood as carbon sinks, wetland generated greenhouse gases may be readily mobilized laterally through hydrologic connectivity between wetlands and adjacent streams (Aho & Raymond, 2019). Our study examined the potential for this mobilization and the fate of dissolved CO_2 in a high-altitude tropical setting and found that the mobilization is rather large and the CO_2 rapidly evaded to the atmosphere.

Tropical wetlands and peatlands are often unaccounted for in Earth system models, despite being recognized as important sources of greenhouse gases to the atmosphere (Page et al., 2011). While high-altitude wetlands remain poorly studied relative to their low altitude counterparts (Chimner & Karberg, 2008), our observations

suggest that—on a per unit area—the upper portion of the stream reach draining this peatland emits more CO₂ to the atmosphere (Figure 3) than tropical wetlands at lower elevations (Sjögersten et al., 2014) or than river waters in the central Amazon (Abril et al., 2014). Rainfall-driven hydrologic variability may amplify or reduce the transport potential among peatlands and streams, but it appears that connectivity between the peatland and the stream allows for the large CO₂ fluxes to the atmosphere. Further investigations should evaluate stream CO₂ evasion during other times of the year (i.e., less rainy months), when peatlands and streams become less connected and stream discharge is considerably reduced across páramos (Correa et al., 2017). Taken together, our findings suggest that high-altitude tropical peatlands (>4,000-m elevation) are important contributors of greenhouse gases to the atmosphere, and given their carbon content, they may play an important role in the global carbon cycle.

4.2. What Are the Mechanisms Driving the Variability in Aquatic CO₂ Fluxes?

At any time and location on the landscape, the molecular concentration of CO₂ can be understood as the balance between biology (production/consumption) and physics (advection/diffusion/evasion). Previous work has shown that the diel dynamics of *pCO₂* in wetlands differs from that of adjacent streams (Riveros-Iregui et al., 2018) and from that of gas-phase CO₂ in upland soils (Riveros-Iregui et al., 2007) due to differences in the magnitude and timing of such biological and physical processes. Our observations corroborate these previous findings (e.g., Figure 5) and suggest that at this high-altitude site, streams are largely carbon “transporters” and peatlands are carbon “transformers” during this time of the year (Figures 2 and 3). It is likely that throughout the year the transforming potential of peatlands and the transport potential between peatlands and streams change as a result of hydrologic connectivity between the peatland and the stream. Peatland-generated CO₂ is mobilized downstream and is subject, primarily, to geomorphic and hydrologic effects that directly influence its concentration. The longitudinal decrease in *pCO₂* is primarily mediated by CO₂ evasion as streams supersaturated with CO₂ tend to reach equilibrium mostly via degassing. Accordingly, our observations suggest that at supersaturated conditions, geomorphic and hydrologic conditions mediate the temporal and spatial efflux of CO₂ but, as equilibrium is reached, hydrologic and geomorphic factors become less important in predicting evasion rate. Thus, we observed that CO₂ evasion in this system is transport-limited (i.e., controlled by flow characteristics, turbulent flow, and water velocity) in the upper portion of the stream, and source limited (i.e., controlled by carbon availability) in the lower portion of the stream. This threshold-like behavior is clearly depicted in Figure 3 as *pCO₂* and flux flatten out at a distance of ~125 m downstream of the peatland. The apparent threshold ranges between 350 and 700 ppm and is likely mediated by atmospheric equilibrium, daily stream conditions, atmospheric pressure, and temperature.

In our study, geomorphic controls on CO₂ evasion appear to be twofold. First, the local slope of the stream channel, which was relatively slight and consistent (<0.08 m/m) for the first ~50 m of the stream reach but progressively increased between 50 and 110 m of the stream reach (up to 0.19 m/m), resulted in a progressive increase in water velocity and turbulence downstream. These hydrologic dynamics are likely responsible for the high CO₂ evasion rates that were accompanied by a rapid drop of *pCO₂* observed through the upper portion of the stream reach (Figure 3). Second, the 4-m waterfall 107 m downstream of the peatland outlet appeared to be the critical final force in the evasion of CO₂, driving equilibrium between *pCO₂* and atmospheric air through the end of the stream reach. While downstream of the waterfall the local slope of the stream channel is lower (average of 0.09 m/m), it appears that once stream *pCO₂* has decreased to close to atmospheric levels no further changes in *pCO₂* occurred—at least during this time of year—likely due to the lack of substantial lateral inputs or not enough in-stream respiration to exceed the CO₂ lost via evasion. Based on our observations, the waterfall accounted for up to 35% of the total evasion observed along the 250-m stream reach, which is comparable to what has been attributed to high slope reaches and waterfalls in other environments (e.g., 36% by Natchimuthu et al., 2017). Waterfalls are very common geomorphic features throughout this steep terrain in the northern Andes, and thus they are likely to be important drivers of *pCO₂* dynamics and the spatial patterns of CO₂ evasion in the region, attenuating variation otherwise controlled by channel slope or hydrologic conditions. Geomorphic features and landscape topography were found to be important drivers of stream *pCO₂* and CO₂ evasion in an arctic region of Sweden (Rocher-Ros et al., 2019). In particular, their study found turbulent reaches were less variable, whereas less turbulent streams supported a broader range of CO₂ concentrations. In our study, high temporal variation, both on

a diel and seasonal scale, is likely the result of connectivity between the peatland and the stream. As peatland water enters the stream channel, it carries with it the diel signal in pCO_2 from photosynthetic and respiratory processes. This diel signal is considerably attenuated by Station 4 (right below the waterfall; Figure 2), likely as a combination of both evasion and in-stream photosynthesis.

In addition to geomorphic controls, an important driver of pCO_2 and CO_2 evasion in the stream was the hydrology itself, namely, discharge and precipitation. Higher discharge resulted in lower pCO_2 in the upper stream reach, likely as a combination of dilution of dissolved CO_2 carried from the peatland into the stream channel and enhanced CO_2 evasion along the stream channel. Large rainfall events flushed peatland CO_2 and resulted in a combined decreased in stream pCO_2 and enhanced CO_2 evasion (Figure 4), which can be observed particularly well for pCO_2 before and after the rainfall event of July 14 (e.g., 13 vs. 16 July). These observations corroborate previous studies (Peter et al., 2014) that reported that large storm events can cause significant impacts that break down diel patterns not only of carbon flux but also other metrics such as discharge, turbidity, pCO_2 , and CDOM and suggest that hydrologic dynamics are important drivers of the timing and magnitude of CO_2 fluxes to the atmosphere in this region.

4.3. How Do CO_2 Fluxes From Terrestrial and Aquatic Environments Compare to One Another in High-Altitude Tropical Catchments?

Our research provides a site-level comparison of CO_2 effluxes from adjacent terrestrial and aquatic landscape elements on a per unit area (and per unit time) basis. Average aquatic flux from the upper stream reach was found to be almost seven times greater than the lower reach of the stream, whereas soil CO_2 efflux from unsaturated soils was found to be almost twice as much as that of saturated soils. The flux from unsaturated soils was slightly larger than the flux from the lower stream reach, while the flux from saturated soils was lower than that of downstream reach. These data support the hypothesis that soil moisture gradient and overall landscape structure are primary drivers of the spatial variability of CO_2 efflux from the terrestrial environments (Riveros-Iregui & McGlynn, 2009). These observations could also support the pulse-shunt hypothesis for aquatic environments and that major hydrologic events may drive the timing and movement of aquatic carbon downstream (Raymond et al., 2016), although additional observations of in-stream carbon processing are required. Nonetheless, our findings expand both concepts by highlighting the magnitude difference (i.e., up to an order of magnitude) between aquatic and terrestrial CO_2 fluxes from adjacent landscape positions. Quantifying this magnitude difference is important because it may help constrain CO_2 effluxes from complex terrain on the basis of landscape structure. Further work should evaluate how seasonal effects, including changes in precipitation, water retention, and connectivity between wetlands and streams, affect the relative magnitude differences between terrestrial and aquatic environments.

Isotopic analyses of the CO_2 degassed from the stream showed that the $\delta^{13}C$ of CO_2 evasion ($\delta^{13}C_{AQ}$) ranged from $-10.9\text{\textperthousand}$ to $-17.2\text{\textperthousand}$ with higher values near the waterfall, likely as a result of turbulent stream dynamics, high degassing rates, and enhanced mixing with atmospheric air (Figure 6). Comparable values (i.e., ranging from $-9.7\text{\textperthousand}$ to $-18.0\text{\textperthousand}$) were found in the $\delta^{13}C$ of soil CO_2 efflux ($\delta^{13}C_S$) from the terrestrial environment (Figure 7), suggesting that CO_2 being emitted from both saturated and unsaturated soil environments may be derived from a similar source. While Páramo vegetation is dominated by C3 plants, our isotopic measurements differ considerably from those to be expected from C3 dominated environments which can be attributed to three plausible explanations. The first explanation relates to the potential contribution from carbonate dissolution and dissolved inorganic carbon from soil processes to $\delta^{13}C_{AQ}$. This phenomenon has been well documented in environments where carbonate is present in the soil or the bedrock (Duvert et al., 2019; Horgby, Boix Canadell, et al., 2019; Horgby, Segatto, et al., 2019). Carbonates are reported to be absent in páramo volcanic soils (Tonneijck et al., 2010), and thus, any dissolved CO_2 would need to be originated in the bedrock. The second explanation involves strong isotopic effects of ongoing CO_2 evasion and methanogenesis, as it has been shown that both processes lead to isotopic enrichment in $\delta^{13}C_{AQ}$ (Campeau et al., 2018; Polsenaere & Abril, 2012; Venkiteswaran et al., 2014; Whiticar, 1999). While we did not measure fluxes of CH_4 , this phenomenon is likely occurring at our site given the carbon content and saturated conditions of soils and therefore future colocated observations of CH_4 fluxes are warranted. The final explanation involves potentially old carbon (i.e., derived from other than recent photosynthate) being respired into the atmosphere, as it has been previously reported that older and deeper carbon may

carry a more enriched isotopic signature than that of recent carbon accumulated in shallow soil (Hicks Pries et al., 2013). This final explanation would also be supported by recent reports from eddy covariance observations that suggest that the Andean Páramo is acting as a net carbon source (Carrillo-Rojas et al., 2019). Future studies should thus examine the ratio between gross primary production and ecosystem respiration of these important carbon stores of the tropics.

The inverse relationship between $\delta^{13}\text{C}_{\text{AQ}}$ and $p\text{CO}_2$ is not entirely surprising (Figure 8). Although not statistically significant in our study, the mixing relationship between $\delta^{13}\text{C}$ and CO_2 has been well examined and described both theoretically and experimentally in previous studies of CO_2 in forest air (e.g., Bowling et al., 2009; Riveros-Iregui, Hu, et al., 2011), soil (e.g., Cerling et al., 1991; Liang et al., 2016), and dissolved CO_2 in aquatic environments (e.g., Campeau et al., 2018; Venkiteswaran et al., 2014). However, to the best of our knowledge, this is the first study to observe this relationship in CO_2 evasion from surface waters of a single stream channel in the context of distance from an aquatic carbon source, namely, the peatland. Our measurements showed that stream locations closer to the peatland outlet had a higher $p\text{CO}_2$ and a more negative $\delta^{13}\text{C}_{\text{AQ}}$, likely because the composition of dissolved CO_2 closer to the peatland outlet was more similar to that of peatland-respired CO_2 and less isotopic fractionation due to degassing or mixing had occurred. Stream locations farther away from the peatland outlet showed a more positive $\delta^{13}\text{C}_{\text{AQ}}$ (and also a greater range in $\delta^{13}\text{C}_{\text{AQ}}$), likely due to evasion-driven fractionation and a longer travel time during which isotopic fractionation can occur. In addition, in-stream photosynthesis may also contribute—and likely more strongly than evasion—to this observed relationship (e.g., Parker et al., 2005; Waldron et al., 2007). Future studies should examine the diel variability of $\delta^{13}\text{C}_{\text{S}}$ to disentangle the effects of evasion from those of photosynthesis. Future studies should also explore the effects of advection and methanogenesis on the $\delta^{13}\text{C}_{\text{AQ}}$ and within a hydrologic context, as this information is required to constrain carbon transformation and fluxes at the catchment scale.

5. Conclusions

Our findings revealed that CO_2 evasion from stream surfaces was up to an order of magnitude greater than soil CO_2 efflux from the adjacent terrestrial environment. Our findings also revealed the importance of hydrologic dynamics in regulating the magnitude and likely fate of dissolved carbon in the stream. While headwater catchments are known to contribute disproportionately larger amounts of carbon to the atmosphere than their downstream counterparts, our study highlights the spatial heterogeneity of CO_2 fluxes within and between aquatic and terrestrial landscape elements in headwater catchments of complex topography.

Stream carbon flux to the atmosphere appeared to be transport limited (i.e., controlled by flow characteristics, turbulent flow, and water velocity) in the upper reaches of the stream draining the peatland, and source limited (i.e., controlled by carbon availability) in the lower reaches of the stream. Thus, proximity to large carbon storage bodies such as wetlands and peatlands, and hydrologic connectivity between wetlands and streams, may mediate the partitioning between lateral (downstream) and vertical (to the atmosphere) fluxes of carbon. A 4-m waterfall along the channel accounted for up to 35% of the total evasion observed along a 250-m stream reach.

Finally, estimates of global carbon budgets are confined by the complexity and heterogeneity of inland landscapes and processes accompanying each (e.g., wetlands, inland waters, and forests; Bodmer et al., 2019; Webb et al., 2019). This heterogeneity often leads to estimates that oversimplify diverse environments, or, inversely, evaluate landscapes elements too independently. Understanding the relationship between carbon flux across terrestrial-aquatic transitions is crucial in the evaluation of the role of headwater streams in the global carbon cycle. Our findings represent a first step in understanding ecosystem carbon cycling at the interface of terrestrial and aquatic ecosystems in high-altitude, tropical, headwater catchments.

Data Availability Statement

All data and code for the reproduction of the analyses presented in this manuscript are freely and publicly available through the University of North Carolina Digital Repository (https://cdr.lib.unc.edu/concern/data_sets/j96026303?locale=en).

Acknowledgments

This work was supported by the National Science Foundation (EAR-1847331). M. H. acknowledges support by NSF Grant ICER-1600506. We would like to thank the staff at the University of San Francisco Quito (USFQ) for logistical support as well as the communities of Cumbayá and Quito, Ecuador. We thank the Ministry of the Environment of Ecuador (research permit 014-018-IC-FLO-DPAN/MA) and the National System of Protected Areas of Ecuador for site access. C. L. S., M. H., and M. L. R. thank everyone in the Carbonshed Lab and the Department of Geography at UNC-Chapel Hill for making this work possible, and for mental and logistical support. A big “thank you” is also needed for the amazing technical support staff at Eosense Inc. and Campbell Scientific, who made this work possible with our frequent phone calls from the field. Finally, two anonymous reviewers and the Editor provided constructive feedback on a previous version of this manuscript.

References

Abril, G., Martinez, J. M., Artigas, L. F., Moreira-Turcq, P., Benedetti, M. F., Vidal, L., et al. (2014). Amazon River carbon dioxide outgassing fuelled by wetlands. *Nature*, 505(7483), 395–398. <https://doi.org/10.1038/nature12797>

Aho, K. S., & Raymond, P. A. (2019). Differential response of greenhouse gas evasion to storms in forested and wetland streams. *Journal of Geophysical Research: Biogeosciences*, 124, 649–662. <https://doi.org/10.1029/2018JG004750>

Allen, G. H., & Pavelsky, T. M. (2018). Global extent of rivers and streams. *Science*, 361(6402), 585–588. <https://doi.org/10.1126/science.aaat0636>

Argerich, A., Haggerty, R., Johnson, S. L., Wondzell, S. M., Dosch, N., Corson-Rikert, H., et al. (2016). Comprehensive multiyear carbon budget of a temperate headwater stream. *Journal of Geophysical Research: Biogeosciences*, 121, 1306–1315. <https://doi.org/10.1002/2015JG003050>

Aufdenkampe, A. K., Mayorga, E., Raymond, P. A., Melack, J. M., Doney, S. C., Alin, S. R., et al. (2011). Riverine coupling of biogeochemical cycles between land, oceans, and atmosphere. *Frontiers in Ecology and the Environment*, 9(1), 53–60. <https://doi.org/10.1890/100014>

Bastviken, D., Tranvik, L. J., Downing, J. A., Crill, P. M., & Enrich-Prast, A. (2011). Freshwater methane emissions offset the continental carbon sink. *Science*, 331(6013), 50–50. <https://doi.org/10.1126/science.1196808>

Battin, T. J., Kaplan, L. A., Findlay, S., Hopkinson, C. S., Marti, E., Packman, A. I., et al. (2008). Biophysical controls on organic carbon fluxes in fluvial networks. *Nature Geoscience*, 1(2), 95–100. <https://doi.org/10.1038/ngeo101>

Benstead, J. P., & Leigh, D. S. (2012). An expanded role for river networks. *Nature Geoscience*, 5(10), 678–679. <https://doi.org/10.1038/ngeo1593>

Bodner, P., Casas-Ruiz, J. P., & del Giorgio, P. A. (2019). Integrating landscape terrestrial and aquatic carbon fluxes. *Eos*, 100. <https://doi.org/10.1029/2019EO135391>

Bowling, D. R., Massman, W. J., Schaeffer, S. M., Burns, S. P., Monson, R. K., & Williams, M. W. (2009). Biological and physical influences on the carbon isotope content of CO₂ in a subalpine forest snowpack, Niwot Ridge, Colorado. *Biogeochemistry*, 95(1), 37–59. <https://doi.org/10.1007/s10533-008-9233-4>

Butman, D., & Raymond, P. A. (2011). Significant efflux of carbon dioxide from streams and rivers in the United States. *Nature Geoscience*, 4(12), 839–842. <https://doi.org/10.1038/ngeo1294>

Buytaert, W., Céller, R., De Bièvre, B., Cisneros, F., Wyseure, G., Deckers, J., & Hofstede, R. (2006). Human impact on the hydrology of the Andean páramos. *Earth-Science Reviews*, 79(1–2), 53–72. <https://doi.org/10.1016/j.earscirev.2006.06.002>

Campeau, A., Bishop, K., Nilsson, M. B., Klemetsson, L., Laudon, H., Leith, F. I., et al. (2018). Stable carbon isotopes reveal soil-stream DIC linkages in contrasting headwater catchments. *Journal of Geophysical Research: Biogeosciences*, 123, 149–167. <https://doi.org/10.1002/2017JG004083>

Carrillo-Rojas, G., Silva, B., Rollenbeck, R., Céller, R., & Bendix, J. (2019). The breathing of the Andean highlands: Net ecosystem exchange and evapotranspiration over the páramo of southern Ecuador. *Agricultural and Forest Meteorology*, 265, 30–47. <https://doi.org/10.1016/j.agrformet.2018.11.006>

Cerling, T. E., Solomon, D. K., Quade, J., & Bowman, J. R. (1991). On the isotopic composition of carbon in soil carbon dioxide. *Geochimica et Cosmochimica Acta*, 55(11), 3403–3405. [https://doi.org/10.1016/0016-7037\(91\)90498-T](https://doi.org/10.1016/0016-7037(91)90498-T)

Chimner, R. A., & Karberg, J. M. (2008). Long-term carbon accumulation in two tropical mountain peatlands, Andes Mountains, Ecuador. *Mires and Peat*, 3(04), 1–10.

Cole, J. J., Prairie, Y. T., Caraco, N. F., McDowell, W. H., Tranvik, L. J., Striegl, R. G., et al. (2007). Plumbing the global carbon cycle: Integrating inland waters into the terrestrial carbon budget. *Ecosystems*, 10(1), 172–185. <https://doi.org/10.1007/s10021-006-9013-8>

Correa, A., Windhorst, D., Tetzlaff, D., Crespo, P., Céller, R., Feyen, J., & Breuer, L. (2017). Temporal dynamics in dominant runoff sources and flow paths in the Andean Páramo. *Water Resources Research*, 53, 5998–6017. <https://doi.org/10.1002/2016WR020187>

Downing, J. A., Cole, J. J., Duarte, C. M., Middelburg, J. J., Melack, J. M., Prairie, Y. T., et al. (2012). Global abundance and size distribution of streams and rivers. *Inland Waters*, 2(4), 229–236. <https://doi.org/10.5268/IW-2.4.502>

Duvert, C., Bossa, M., Tyler, K. J., Wynn, J. G., Munksgaard, N. C., Bird, M. I., et al. (2019). Groundwater-derived DIC and carbonate buffering enhance fluvial CO₂ evasion in two Australian tropical rivers. *Journal of Geophysical Research: Biogeosciences*, 124, 312–327. <https://doi.org/10.1029/2018JG004912>

Hicks Pries, C. E., Schuur, E. A., & Crummer, K. G. (2013). Thawing permafrost increases old soil and autotrophic respiration in tundra: Partitioning ecosystem respiration using $\delta^{13}\text{C}$ and $\Delta^{14}\text{C}$. *Global Change Biology*, 19(2), 649–661. <https://doi.org/10.1111/gcb.12058>

Horgby, Å., Boix Canadell, M., Ulseth, A. J., Vennemann, T. W., & Battin, T. J. (2019). High-resolution spatial sampling identifies groundwater as driver of CO₂ dynamics in an Alpine stream network. *Journal of Geophysical Research: Biogeosciences*, 124, 1961–1976. <https://doi.org/10.1029/2019JG005047>

Horgby, Å., Segatto, P. L., Bertuzzo, E., Lauerwald, R., Lehner, B., Ulseth, A. J., et al. (2019). Unexpected large evasion fluxes of carbon dioxide from turbulent streams draining the world’s mountains. *Nature Communications*, 10(1), 4888–4889. <https://doi.org/10.1038/s41467-019-12905-z>

Hotchkiss, E. R., Hall, R. O. Jr., Sponseller, R. A., Butman, D., Klaminder, J., Laudon, H., et al. (2015). Sources of and processes controlling CO₂ emissions change with the size of streams and rivers. *Nature Geoscience*, 8(9), 696–699. <https://doi.org/10.1038/ngeo2507>

Hribiljan, J. A., Suárez, E., Bourgeau-Chavez, L., Endres, S., Lilleskov, E. A., Chimbolema, S., et al. (2017). Multidate, multisensor remote sensing reveals high density of carbon-rich mountain peatlands in the páramo of Ecuador. *Global Change Biology*, 23(12), 5412–5425. <https://doi.org/10.1111/gcb.13807>

Hribiljan, J. A., Suárez, E., Heckman, K. A., Lilleskov, E. A., & Chimner, R. A. (2016). Peatland carbon stocks and accumulation rates in the Ecuadorian páramo. *Wetlands Ecology and Management*, 24(2), 113–127. <https://doi.org/10.1007/s11273-016-9482-2>

Johnson, M. S., Billett, M. F., Dinsmore, K. J., Wallin, M., Dyson, K. E., & Jassal, R. S. (2010). Direct and continuous measurement of dissolved carbon dioxide in freshwater aquatic systems—Method and applications. *Ecohydrology*, 3(1), 68–78. <https://doi.org/10.1002/eco.95>

Liang, L. L., Riveros-Iregui, D. A., & Risk, D. A. (2016). Spatial and seasonal variabilities of the stable carbon isotope composition of soil CO₂ concentration and flux in complex terrain. *Journal of Geophysical Research: Biogeosciences*, 121, 2328–2339. <https://doi.org/10.1002/2015JG003193>

Luteyn, J. L. (1999). *Páramos: A checklist of plant diversity, geographical distribution, and botanical literature* (pp. 1–278). Bronx, NY: New York Botanical Garden Press.

Natchimuthu, S., Wallin, M., Klemedtsson, L., & Bastviken, D. (2017). Spatio-temporal patterns of stream methane and carbon dioxide emissions in a hemiboreal catchment in Southwest Sweden. *Scientific Reports*, 7(1), 39,729. <https://doi.org/10.1038/srep39729>

Pacific, V. J., Jencso, K. G., & McGlynn, B. L. (2010). Variable flushing mechanisms and landscape structure control stream DOC export during snowmelt in a set of nested catchments. *Biogeochemistry*, 99(1-3), 193–211. <https://doi.org/10.1007/s10533-009-9401-1>

Pacific, V. J., McGlynn, B. L., Riveros-Iregui, D. A., Welsch, D. L., & Epstein, H. E. (2008). Variability in soil respiration across riparian-hillslope transitions. *Biogeochemistry*, 91(1), 51–70. <https://doi.org/10.1007/s10533-008-9258-8>

Page, S. E., Rieley, J. O., & Banks, C. J. (2011). Global and regional importance of the tropical peatland carbon pool. *Global Change Biology*, 17(2), 798–818. <https://doi.org/10.1111/j.1365-2486.2010.02279.x>

Parker, S. R., Poulsen, S. R., Gammons, C. H., & DeGrandpre, M. D. (2005). Biogeochemical controls on diel cycling of stable isotopes of dissolved O₂ and dissolved inorganic carbon in the Big Hole River, Montana. *Environmental Science & Technology*, 39(18), 7134–7140. <https://doi.org/10.1021/es0505595>

Peter, H., Singer, G. A., Preiler, C., Chifflard, P., Steniczka, G., & Battin, T. J. (2014). Scales and drivers of temporal pCO₂ dynamics in an Alpine stream. *Journal of Geophysical Research: Biogeosciences*, 119, 1078–1091. <https://doi.org/10.1002/2013JG002552>

Polsenaere, P., & Abril, G. (2012). Modelling CO₂ degassing from small acidic rivers using water pCO₂, DIC and δ¹³C-DIC data. *Geochimica et Cosmochimica Acta*, 91, 220–239. <https://doi.org/10.1016/j.gca.2012.05.030>

Raymond, P. A., Hartmann, J., Lauerwald, R., Sobek, S., McDonald, C., Hoover, M., et al. (2013). Global carbon dioxide emissions from inland waters. *Nature*, 503(7476), 355–359. <https://doi.org/10.1038/nature12760>

Raymond, P. A., Sayers, J. E., & Sobczak, W. V. (2016). Hydrological and biogeochemical controls on watershed dissolved organic matter transport: Pulse-shun concept. *Ecology*, 97(1), 5–16. <https://doi.org/10.1890/14-1684.1>

Risk, D., Nickerson, N., Creelman, C., McArthur, G., & Owens, J. (2011). Forced diffusion soil flux: A new technique for continuous monitoring of soil gas efflux. *Agricultural and Forest Meteorology*, 151(12), 1622–1631. <https://doi.org/10.1016/j.agrformet.2011.06.020>

Riveros-Iregui, D. A., Covino, T. P., & González-Pinzón, R. (2018). The importance of and need for rapid hydrologic assessments in Latin America. *Hydrological Processes*, 32(15), 2441–2451. <https://doi.org/10.1002/hyp.13163>

Riveros-Iregui, D. A., Emanuel, R. E., Muth, D. J., McGlynn, B. L., Epstein, H. E., Welsch, D. L., et al. (2007). Diurnal hysteresis between soil CO₂ and soil temperature is controlled by soil water content. *Geophysical Research Letters*, 34, L17404. <https://doi.org/10.1029/2007GL030938>

Riveros-Iregui, D. A., & McGlynn, B. L. (2009). Landscape structure control on soil CO₂ efflux variability in complex terrain: Scaling from point observations to watershed scale fluxes. *Journal of Geophysical Research: Biogeosciences*, 114, G02010. <https://doi.org/10.1029/2008JG000885>

Riveros-Iregui, D. A., Hu, J., Burns, S. P., Bowling, D. R., & Monson, R. K. (2011). An interannual assessment of the relationship between the stable carbon isotopic composition of ecosystem respiration and climate in a high-elevation subalpine forest. *Journal of Geophysical Research*, 116, G02005. <https://doi.org/10.1029/2010JG001556>

Riveros-Iregui, D. A., McGlynn, B. L., Marshall, L. A., Welsch, D. L., Emanuel, R. E., & Epstein, H. E. (2011). A watershed-scale assessment of a process soil CO₂ production and efflux model. *Water Resources Research*, 47, W00J04. <https://doi.org/10.1029/2010WR009941>

Rocher-Ros, G., Sponseller, R. A., Lidberg, W., Mörth, C.-M., & Giesler, R. (2019). Landscape process domains drive patterns of CO₂ evasion from river networks. *Limnology and Oceanography Letters*, 4, 87–95. <https://doi.org/10.1002/lol2.10108>

Sánchez, M. E., Chimner, R. A., Hribljan, J. A., Lilleskov, E. A., & Suárez, E. (2017). Carbon dioxide and methane fluxes in grazed and undisturbed mountain peatlands in the Ecuadorian Andes. *Mires and Peat*, 19(20), 1–18. <https://doi.org/10.19189/MaP.2017.OMB.277>

Schelker, J., Singer, G. A., Ulseth, A. J., Hengsberger, S., & Battin, T. J. (2016). CO₂ evasion from a steep, high gradient stream network: Importance of seasonal and diurnal variation in aquatic pCO₂ and gas transfer. *Limnology and Oceanography*, 61(5), 1826–1838. <https://doi.org/10.1002/lo.10339>

Sjögersten, S., Black, C. R., Evers, S., Hoyos-Santillan, J., Wright, E. L., & Turner, B. L. (2014). Tropical wetlands: A missing link in the global carbon cycle? *Global Biogeochemical Cycles*, 28, 1371–1386. <https://doi.org/10.1002/2014GB004844>

Sklenář, P., & Lægaard, S. (2003). Rain-shadow in the high Andes of Ecuador evidenced by paramo vegetation. *Arctic, Antarctic, and Alpine Research*, 35(1), 8–17. [https://doi.org/10.1657/1523-0430\(2003\)035\[0008:RSITHA\]2.0.CO;2](https://doi.org/10.1657/1523-0430(2003)035[0008:RSITHA]2.0.CO;2)

Stanley, E. H., & del Giorgio, P. A. (2018). Toward an integrative, whole network approach to C cycling of inland waters. *Limnology and Oceanography Letters*, 3(3), 39–40. <https://doi.org/10.1002/lol2.10085>

Tonneijck, F. H., Jansen, B., Nierop, K. G. J., Verstraten, J. M., Sevink, J., & de Lange, L. (2010). Towards understanding of carbon stocks and stabilization in volcanic ash soils in natural Andean ecosystems of northern Ecuador. *European Journal of Soil Science*, 61(3), 392–405. <https://doi.org/10.1111/j.1365-2389.2010.01241.x>

Vannote, R. L., Minshall, G. W., Cummins, K. W., Sedell, J. R., & Cushing, C. E. (1980). The river continuum concept. *Canadian Journal of Fisheries and Aquatic Sciences*, 37(1), 130–137. <https://doi.org/10.1139/F80-017>

Venkiteswaran, J. J., Schiff, S. L., & Wallin, M. B. (2014). Large carbon dioxide fluxes from headwater boreal and sub-boreal streams. *PLoS ONE*, 9(7), e101756. <https://doi.org/10.1371/journal.pone.0101756>

Waldron, S., Scott, E. M., & Soulsby, C. (2007). Stable isotope analysis reveals lower-order river dissolved inorganic carbon pools are highly dynamic. *Environmental Science & Technology*, 41(17), 6156–6162. <https://doi.org/10.1021/es0706089>

Ward, N. D., Bianchi, T. S., Medeiros, P. M., Seidel, M., Richey, J. E., Keil, R. G., & Sawakuchi, H. O. (2017). Where carbon goes when water flows: Carbon cycling across the aquatic continuum. *Frontiers in Marine Science*, 4, 7. <https://doi.org/10.3389/fmars.2017.00007>

Webb, J. R., Santos, I. R., Maher, D. T., & Finlay, K. (2019). The importance of aquatic carbon fluxes in net ecosystem carbon budgets: A catchment-scale review. *Ecosystems*, 22(3), 508–527. <https://doi.org/10.1007/s10021-018-0284-7>

Whiticar, M. J. (1999). Carbon and hydrogen isotope systematics of bacterial formation and oxidation of methane. *Chemical Geology*, 161(1–3), 291–314. [https://doi.org/10.1016/s0009-2541\(99\)00092-3](https://doi.org/10.1016/s0009-2541(99)00092-3)